CHIN. PHYS. LETT. Vol. 36, No. 10 (2019) 105201

Generation of Ultrahigh-Velocity Collisionless Electrostatic Shocks Using an Ultra-Intense Laser Pulse Interacting with Foil-Gas Target *

Shu-Kai He(贺书凯)[1], Jin-Long Jiao(矫金龙)[2**], Zhi-Gang Deng(邓志刚)[1], Feng Lu(卢峰)[1], Lei Yang(杨雷)[1], Fa-Qiang Zhang(张发强)[1], Ke-Gong Dong(董克攻)[1], Wei Hong(洪伟)[1], Zhi-Meng Zhang(张智猛)[1], Bo Zhang(张博)[1], Jian Teng(滕建)[1], Wei-Min Zhou(周维民)[1], Yu-Qiu Gu(谷渝秋)[1]

[1]*Science and Technology on Plasma Physics Laboratory, Research Center of Laser Fusion, China Academy of Engineering Physics, Mianyang 621900*
[2]*School of Physics, Peking University, Beijing 100871*

(Received 22 May 2019)

Ultra high-velocity collisionless shocks are generated using an ultra-intense laser interacting with foil-gas target, which consists of copper foil and helium gas. The energy of helium ions accelerated by shock and the proton probing image of the shock electrostatic field show that the shock velocity is 0.02c, where c is the light speed. The numerical and theory studies indicate that the collisionless shock velocity exceeding 0.1c can be generated by a laser pulse with picosecond duration and an intensity of 10^{20} W/cm^2. This system may be relevant to the study of mildly relativistic velocity collisionless shocks in astrophysics.

PACS: 52.38.−r, 52.38.Kd, 52.65.Rr DOI: 10.1088/0256-307X/36/10/105201

The ultra high-velocity collisionless shocks in unmagnetic plasmas are ubiquitous in the fields of astrophysics and laser plasma physics.[1,2] In astrophysics, for example, the velocity of collisionless shocks generated when a type-Ibc supernova remnant blast shell propagates into the interstellar medium can generally reach $0.1c$ (where c is the light speed) or even $0.6c$ (SN 2009bb).[3] Such mildly relativistic shocks are also common to the afterglows of gamma-ray bursts (GRBs), blazar jets and microquasars.[4] Several works show that collisionless shocks can also be generated in laser-plasma experiments in the laboratory and are relevant to astrophysics processes through transformation and similarity criteria.[5−10] However, most of these works are devoted to nonrelativistic velocity shocks. In contrast, there are few studies on the generation of mildly relativistic velocity collisionless shocks by laser plasma experiments in the laboratory.

In this Letter, we present the experimental observation of ultrahigh-velocity collisionless shocks and the subsequent ion acceleration by an ultra-intense laser interacting with foil-gas target, which consists of copper foil and helium gas. The collisionless shocks are generated following the sudden expansion of hot dense plasma into a rarefied ionized medium.[11−13] The hot dense plasma is produced from the interaction of an ultra-intense (intensity excess 10^{18} W/cm^2) 0.8-ps laser with the front surface of the copper foil. The rear surface of the copper foil will collapse and expand into helium gas. The electrostatic field in the shock region can accelerate helium ions to twice the shock velocity. The shocks are observed using a laser-accelerated proton beam as a charged particle probe. The accelerated helium ions are recorded by a Thomson parabola spectrometer. The relationship between the shock velocity and the experimental conditions is investigated by a series of particle-in-cell (PIC) simulations and a theory model. This relationship indicates that mildly relativistic velocity collisionless shocks can be generated from the interaction of a state-of-the-art laser facility with a foil-gas target.

The experiment was performed using the Xing-Guang Ⅲ laser facility at the Science and Technology in the Plasma Physics Laboratory. The experimental setup is similar to one of our published works.[14] A 0.8-ps, 100-J laser pulse (ps laser in Fig. 1) was focused at an intensity about 5×10^{18} W/cm^2 onto a 7-μm-thick copper foil (interaction target in Fig. 1). A nozzle with 1-mm diameter behind the interaction target can support a helium gas jet with an electron density of 5×10^{19}/cm^3, which is simulated by the computational fluid dynamics program FLUENT. The distance between the interaction target and the nozzle center is 1 mm. The energy spectrum of ions at the normal of the interaction target rear surface was measured with a Thomson parabola ion spectrometer, which enables ions with different charge-to-mass ratios to be distinguished since they produce unique parabolic trajectories at the detector plane. The spectrometer was positioned 40 cm from the interaction region. A 200-μm-diameter pinhole served as the entrance to the spectrometer, which subtended a solid angle of 2×10^{-7} steradians. The ions were recorded using a Fuji film image plate (IP). The energy spectrum of the hot electrons in front of the interaction target was measured using an electron magnetic spectrometer with 2000 G. The thin target used in our experiments has slight influence on the transmission of electrons, thus the hot electron temperature in front of the target is basically the same as that behind the target. The plasma evolution was monitored by pro-

*Supported by the Science Challenge Project under Grant Nos TZ2018005 and TZ2016005, and the National Key Research and Development Program of China under Grant No 2016YFA0401100.
**Corresponding author. Email: jiao.jl@foxmail.com
© 2019 Chinese Physical Society and IOP Publishing Ltd

ton radiographs. The probing proton beam was externally generated from the interaction of a 30-fs 10-J laser pulse at an intensity in excess of 10^{18} W/cm^2 (fs laser in Fig. 1) with a 25-μm aluminum foil (proton target in Fig. 1). The probing proton beam was recorded on a stack of radiochromic films (RCF) with 6-μm aluminum foil on the front surface to shield x-rays and electrons. The distance between the proton target and the nozzle center was $l = 6.5$ mm, and the distance between the RCF stack and the nozzle center was $L = 60$ mm, which yielded a projection magnification $M = (L + l)/l = 10$. In experiments, the fs laser pulse arrived at the proton target 200 ps before the ps laser arrived at the interaction target.

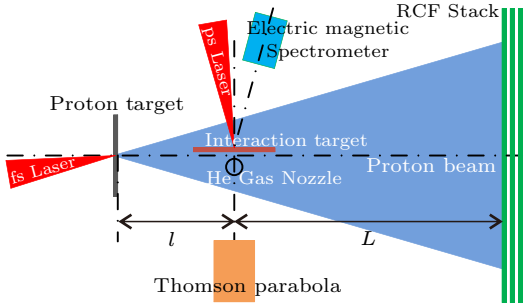

Fig. 1. The experimental layout of the ultrahigh-velocity shock generation and diagnosis. Here $L = 60$ mm and $l = 6.5$ mm, which yields a projection magnification $M = (L + l)/l = 10$. Both laser pulses are incident at 5° from the normal of the targets.

Figure 2 shows the main experimental results. To identify the helium ion signal, we performed two experiments with and without helium gas. The IP figures of the two experiments are Figs. 2(a) and 2(b). C^{3+} and He^{1+} have identical charge-to-mass ratios, and so do C^{6+} and He^{2+}. The ions with the same charge-to-mass ratios are in identical parabola lines as measured by the Thomson parabola spectrometer. Figure 2(b) shows that the signals of C^{3+} and C^{6+} are notably weak in the laser copper foil interaction. At the same positions, the signal intensity becomes obvious when the laser foil-gas target interaction occurs as shown in Fig. 2(a), which implies that the strong signals mainly come from helium ions. The He^{2+} spectra (blue solid line in Fig. 3) show a plateau structure at approximately 3 MeV, which is a characteristic of ions accelerated by collisionless shock waves.[15,16] The hot electron temperature at the front surface of the interaction target obtained from the electron magnetic spectrometer, is about 0.8 MeV (Fig. 2(c)). Thus, the helium plasma ion acoustic velocity can be estimated as $c_s = \sqrt{\frac{ZT_e}{m_i}} = 0.02c$. Assuming that helium ions are reflected by the collisionless shock with twice the ion acoustic velocity, the helium ion energy can reach 3 MeV, which is consistent with Fig. 3. The distance between the interaction target and the shock region is 1.4 mm according to the RCF image considering the projection magnification (Fig. 2(d)). The proton energy corresponding to Fig. 2(d) is larger than 0.7 MeV as calculated by the Monte Carlo code SRIM[17] and smaller than 1.5 MeV as measured by the Thomson parabola ion spectrometer in another shot. Considering the delay time (200 ps) between two laser pulses, we can obtain the shock velocity of $v_{sh} = 0.013-0.026c$, which means that the shock Mach number is about $\mathrm{Ma} = v_{sh}/c_s \sim 1$. These results suggest that the ultrahigh-velocity collisionless shock with $0.02c$ was generated in our experiment. We note that this is the first experimental evidence for collisionless shock ion acceleration characteristics since the shock electrostatic field structure and ion signals were simultaneously observed.

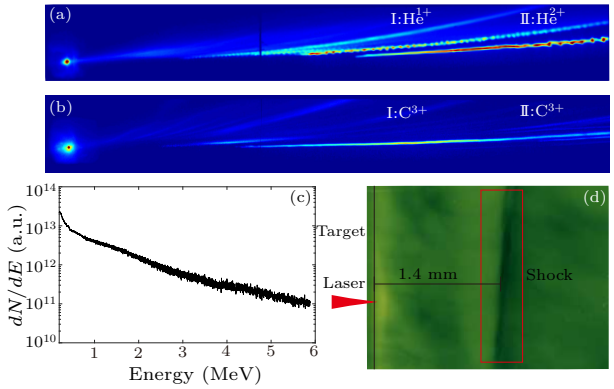

Fig. 2. Experimental results. Contrast experiments with (a) and without (b) helium gas. (c) Energy spectra of electrons at front surface of copper foil. (d) Proton probing RCF image.

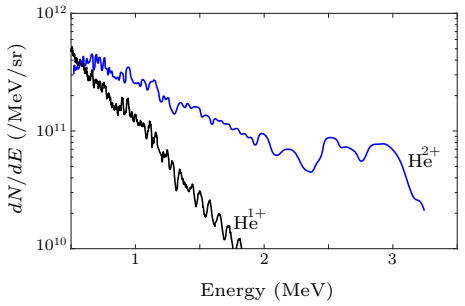

Fig. 3. He^{1+} and He^{2+} energy spectra reconstructed from Fig. 2(a).

The shock structure observed in our experiment is collisionless. We estimate the ion-ion collision mean free path in helium gas and compare it with the measured shock region width. We assume that the helium gas is fully ionized, which corresponds to the minima for the ion-ion mean free path and consequently the most collisional case. The Coulomb logarithm is $\ln\Lambda = \ln(\frac{4\pi(\varepsilon_0\kappa_B T_e)^{1.5}}{(Ze)^3 n^{0.5}})$,[18] where n is the helium plasma ion density, T_e is the hot electrons temperature, Z is the ionization state of the helium plasma, and e is the elementary electric charge. In our experiments, when $n = 5 \times 10^{19}$/cm^3, $k_B T_e = 0.8$ MeV, $Z = 2$, the Coulomb logarithm is $\ln\Lambda = 18$. We use the formula for the ion-ion mean free path $\lambda_{ii} = \frac{4\pi\varepsilon_0^2 m_i^2 v^4}{e^4 Z^4 n \ln\Lambda}$,[19] where m_i is the helium ion mass, v is the shock velocity. When $m_i = 6.68 \times 10^{-27}$ kg and $v = 0.02c$, the ion-ion mean free path is estimated to be 6 m. The width of the shock region, which is ob-

tained from Fig. 2(d) by measuring the width of the high-density proton region, is approximately 0.1 mm. Since the width of the shock region is much shorter than the ion-ion mean free path, the observed shock structure in our experiment is collisionless.

To study the ultrahigh-velocity shock formation under the laboratory conditions, we use one- (1D) and two-dimensional (2D) simulations with the full electromagnetic relativistic PIC code EPOCH.[20] In the 1D PIC simulation, we model the interaction of two proton plasmas with identical electron temperatures and different electron densities. At $t = 0$, there is no relative drift between the two plasmas. The length of the simulation box is L, plasma 0, whose electron density is $0.1n_c$ ($n_c = 1.12 \times 10^{21}\,\mathrm{cm}^{-3}$), occupies the right-hand half ($L/2 < x < L$), whereas plasma 1, whose electron density is $1.0n_c$, occupies the left-hand half ($0 < x < L/2$). Both electrons and protons follow a Maxwellian velocity distribution, and their temperatures are 2 MeV and 100 eV, respectively. The box length $L = 200\,\mu\mathrm{m}$ is divided into 50000 cells. We use 100 macro-particles per cell per species with current smoothing for good accuracy. Both the left-hand and right-hand boundaries are perfectly reflecting walls for the particles.

Figure 4(a) shows several shock features, which have been discussed by He *et al.*[21,22] and Chen *et al.*[23] These features will be used to construct our theoretical model. (i) The plasma system has five typical regions according to the profiles of electron density and ion momentum. Regions 1 and 5 are the unperturbed part of plasmas 1 and 0, respectively. The plasma density is uniform in these two regions. Region 2 is the rarefaction wave because of the expansion of plasma 1 into plasma 0 with an exponentially decreasing density profile, the corresponding ion momentum linearly increases. The shock downstream can be divided into two regions according to different ion species, and we assign them as regions 3 and 4. (ii) Region 3 acts as a piston on region 4, thus the average velocities of ions in regions 3 and 4 are approximately equal.

We can build a model to estimate the shock velocity according to the shock features discussed above. Ignoring the ions reflected by shock, we describe the plasmas using 1D two-fluid equations[24]

$$\partial n_\mathrm{i}/\partial t + \partial(n_\mathrm{i}v_\mathrm{i})/\partial x = 0, \tag{1}$$

$$\partial P_\mathrm{e}/\partial x + en_\mathrm{e}E = 0, \tag{2}$$

$$m_\mathrm{i}(\partial v_\mathrm{i}/\partial t + v_\mathrm{i}\partial v_\mathrm{i}/\partial x) = ZeE, \tag{3}$$

where n_i, v_i, m_i, P_e, n_e, E, e and Z are the plasma ion density, ion velocity, ion mass, electron pressure, electron density, electric field intensity, elementary charge, and ionization degree, respectively. We can obtain a relationship from Eqs. (1)–(3),

$$v_\mathrm{i}/c_\mathrm{s} \pm \ln(n_\mathrm{i}/n_0) = \text{const.}, \tag{4}$$

where v_i is the plasma ion velocity, n_i is the ion density, c_s is the ion acoustic velocity, and n_0 is the initial ion density.

The average ion velocities of regions 3 and 4 can be obtained by applying Eq. (4) to regions 1 and 3–5. They are (we assign the ion average velocities of regions 3 and 4 as $v_{\mathrm{d}1}$ and $v_{\mathrm{d}0}$),

$$v_{\mathrm{d}1} = c_{\mathrm{s}1}\ln(n_{\mathrm{e}1}/n_m),\ v_{\mathrm{d}0} = c_{\mathrm{s}0}\ln(n_m/n_{\mathrm{e}0}), \tag{5}$$

where $c_{\mathrm{sl}}^2 = Z_lT/A_lm_\mathrm{p}$, $l = 0, 1$, $T = \frac{1}{3}(\bar{\varepsilon}^2 + 2m_\mathrm{e}c^2\bar{\varepsilon})/(\bar{\varepsilon} + m_\mathrm{e}c^2)$, $\bar{\varepsilon} = \frac{3}{2}k_\mathrm{B}T_\mathrm{e}$, m_p is the proton mass. The ions in regions 3 and 4 have identical average velocities because plasma 1 pushes plasma 0, while we assume that the shock velocity approximately equals the shock downstream ion velocity; i.e., $v_{\mathrm{d}1} = v_{\mathrm{d}0} = v_{\mathrm{sh}}$. Thus, we obtain

$$v_{\mathrm{sh}} = \frac{\alpha_0\alpha_1}{\alpha_0 + \alpha_1}(T/m_\mathrm{p})^{1/2}\ln\Gamma, \tag{6}$$

where $\alpha_l = (Z_l/A_l)^{1/2}$ and $\Gamma = n_{\mathrm{e}1}/n_{\mathrm{e}0}$. When we consider a laser pulse in this plasma system, the hot electrons temperature can be estimated using Wilks' scale law, $k_\mathrm{B}T_\mathrm{e} = 0.511 \times (\sqrt{1 + a_0^2} - 1)$.[25]

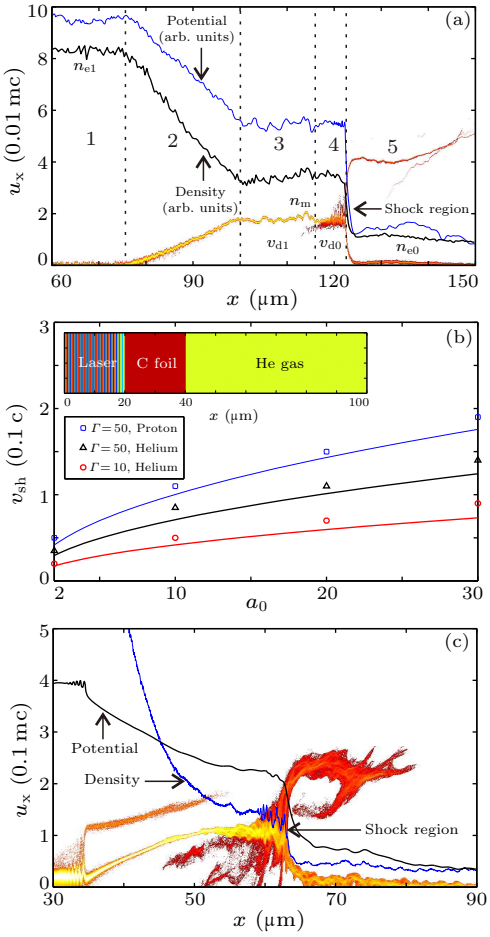

Fig. 4. (a) The 1D PIC simulation result. The black solid line is plasma density and the blue solid line is plasma potential. (b) Scaling of the shock velocity with laser a_0. The markers are the PIC simulation cases. The inset is the 2D PIC simulation setting. The solid lines are the results of Eq. (6). (c) The results in the case of $a_0 = 10$, $\Gamma = 50$ and hydrogen gas at $t = 0.9$ ps.

To confirm Eq. (6), we simulate the interaction of an ultra-intense laser pulse with a foil-gas com-

plex target. The laser is polarized along the Y direction, propagates along the X direction and has a wavelength of 1 μm. We have simulated different laser intensities, which correspond to a normalized laser vector potential a_0 of 2–30. The simulation box is $X \times Y = 100\,\mu\text{m} \times 20\,\mu\text{m}$ with a cell size of $dX \times dY = 0.033\,\mu\text{m} \times 0.033\,\mu\text{m}$. The dense carbon slab is located at $x = 20$–$40\,\mu\text{m}$, and the helium gas is a slab at $x = 40$–$100\,\mu\text{m}$ (inset in Fig. 4(b)). The entire target is fully ionized, and the electron density of the gas is fixed to $0.1n_c$, whereas the electron density of the carbon slab is $a_0 n_c$. The two plasmas have identical initial electron temperatures of 200 eV and ion temperatures of 20 eV. The boundaries for the electromagnetic field are absorptive in the X direction and periodic in the Y direction. The boundaries for the particles are periodic in the Y direction, absorptive on the left-hand side of the X direction and thermal on the right-hand side. The thermal boundary is that the particles are re-emitted into box with an initial thermal velocity when they arrive at the box boundaries.

The shock velocities obtained from 2D simulations and Eq. (6) are consistent as shown in Fig. 4(b). When $a_0 = 2$, the corresponding laser intensity is similar with our experimental conditions. The shock velocity under this laser intensity is about $0.02c$–$0.03c$ (helium gas), which is in good agreement with our experimental results. For higher laser intensity, a collisionless shock with propagation velocity of $0.1c$ can be generated by a laser pulse with intensity of $10^{20}\,\text{W/cm}^2$ ($a_0 = 10$, hydrogen gas), as shown in Fig. 4(c).

In conclusion, high-energy ion signals measured by the Thomson parabola ion spectrometer and collisionless shock electrostatic field structure measured by the RCF stack are simultaneously observed using the ultra-intense laser interacting with foil-gas target. The experimental results indicate that ultrahigh-velocity collisionless shocks with $0.02c$ are generated. The relationship between the shock velocity and the experimental conditions, which is investigated using a series of PIC simulations and a theory model, shows that a mildly relativistic velocity collisionless shock can be generated by a state-of-the-art laser facility that interacts with a foil-gas target. These results are potentially interesting for the laboratory study of mildly relativistic velocity collisionless shocks, which is relevant to the understanding of important astrophysical situations.

References

[1] Esirkepov T Z and Bulanov S V 2012 *EAS Publ. Ser.* **58** 7

[2] Bulanov S V, Esirkepov T Z, Kando M, Kogaa J, Kondoa K and Kornc G 2015 *Plasma Phys. Rep.* **41** 1

[3] Soderberg A M, Chakraborti S, Pignata G, Chevalier R A, Chandra P, Ray A, Wieringa M H, Copete A, Chaplin V, Connaughton V, Barthelmy S D, Bietenholz M F, Chugai N, Stritzinger M D, Hamuy M, Fransson C, Fox O, Levesque E M, Grindlay J E, Challis P, Foley R J, Kirshner R P, Milne P A and Torres M A P 2010 *Nature* **463** 513

[4] Committee W O P A 2010 *Research Opportunities in Plasma Astrophysics: Report of the Workshop on Opportunities in Plasma Astrophysics* (Patti Wieser, Princeton Plasma Physics Laboratory, Princeton Plasma Physics Lab. (PPPL), Princeton, NJ (United States) pMedium: ED)

[5] Drake R P 2000 *Phys. Plasmas* **7** 4690

[6] Romagnani L, Bulanov S V, Borghesi M, Audebert P, Gauthier J G, Lowenbruck K, Mackinnon A J, Patel P, Pretzler G, Toncian T and Willi O 2008 *Phys. Rev. Lett.* **101** 025004

[7] Nilson P M, Willingale L, Kaluza M C, Kaluza M C, Thomas A G R, Tatarakis M, Najmudin Z, Clarke R J, Lancaster K L, Karsch S, Schreiber J, Evans R G, Dangor A E and Krushelnick K 2006 *Phys. Rev. Lett.* **97** 255001

[8] Ahmed H, Dieckmann M E, Romagnani L, Doria D, Sarri G, Cerchez M, Ianni E, Kourakis I, Giesecke A L, Notley M, Prasad R, Quinn K, Willi O and Borghesi M 2013 *Phys. Rev. Lett.* **110** 205001

[9] Kuramitsu Y, Sakawa Y, Morita T, Gregory C D, Pikuz S A, Loupias B, Koenig M, Waugh J N, Woolsey N, Morita T, Moritaka T, Sano T, Matsumoto Y, Mizuta A, Ohnishi N and Takabe H 2011 *Phys. Rev. Lett.* **106** 175002

[10] Liu X, Li Y T, Zhang Y, Zhong J Y, Zheng W D, Dong Q L, Chen M, Zhao G, Sakawa Y, Morita T, Kuramitsu Y, Kato T N, Chen L M, Lu X, Ma J L, Wang W M, Sheng Z M, Takabe H, Rhee Y J, Ding Y K, Jiang S E, Liu S Y, Zhu J Q and Zhang J 2011 *New J. Phys.* **13** 093001

[11] Sarri G, Dieckmann M E, Kourakis I and Borghesi M 2011 *Phys. Rev. Lett.* **107** 025003

[12] Sarri G, Dieckmann M E, Kourakis I and Borghesi M 2010 *Phys. Plasmas* **17** 082305

[13] Dieckmann M E, Sarri G, Romagnani L, Kourakis I and Borghesi M 2010 *Plasma Phys. Control. Fusion* **52** 025001

[14] Jiao J L, He S K, Deng Z G, Lu F, Zhang Y, Yang L, Zhang F Q, Dong K G, Wang S Y, Zhang B, Teng J, Hong W and Gu Y Q 2017 *Acta Phys. Sin.* **66** 085201 (in Chinese)

[15] Silva L O, Marti M, Davies J R and Fonseca R A 2004 *Phys. Rev. Lett.* **92** 015002

[16] Wei M S, Mangles S P D, Najmudin Z, Walton B, Gopal A, Tatarakis M, Dangor A E, Clark E L, Evans R G, Fritzler S, Clarke R J, Hernandez-Gomez C, Neely D, Mori W, Tzoufras M and Krushelnick K 2004 *Phys. Rev. Lett.* **93** 155003

[17] Ziegler J F 1999 *J. Appl. Phys.* **85** 1249

[18] Lyman S 1963 *Phys. Fully Ionized Gases* (New York: Wiley) vol 139 p 1045

[19] Chenais-Popovics C, Renaudin P, Rancu O, Gilleron F and Gauthier J C 1997 *Phys. Plasmas* **4** 190

[20] Brady C S and Arber T D 2011 *Plasma Phys. Control. Fusion* **53** 015001

[21] He M Q, Dong Q L, Sheng Z M, Weng S M, Chen M, Wu H C and Zhang J 2007 *Phys. Rev. E* **76** 035402

[22] He M Q, Shao X, Liu C S, Liu T C, Su J J, Dudnikova G, Sagdeev R Z and Sheng Z M 2012 *Phys. Plasmas* **19** 073116

[23] Chen M, Sheng Z M, Dong Q L, He M Q, Li Y T, Bari M A and Zhang J 2007 *Phys. Plasmas* **14** 053102

[24] Eliezer S 2002 *The Interaction of High-Power Lasers with Plasmas* (Boca Raton: CRC Press)

[25] Wilks S C, Kruer W L, Tabak M and Langdon A B 1992 *Phys. Rev. Lett.* **69** 1383